Noname manuscript No.
(will be inserted by the editor)

Nonlocal structure of the leading order *ab initio* effective potentials for proton elastic scattering from light nuclei

Ch. Elster · M. Burrows · R.B. Baker · S.P. Weppner · K.D. Launey · P. Maris · G. Popa

Received: date / Accepted: date

Abstract Based on the spectator expansion of the multiple scattering series we employ a chiral next-to-next-to-leading order (NNLO) nucleon-nucleon interaction on the same footing in the structure as well as in the reaction calculation to obtain an in leading-order consistent effective potential for nucleon-nucleus elastic scattering, which includes the spin of the struck target nucleon. As an example we present proton scattering off ^{12}C.

Keywords Nucleon-Nucleus Scattering · *Ab Initio* Effective Potentials

PACS 24.10.-i · 24.10.Ht · 25.40.-h · 25.40.Cm

1 Introduction

Recent developments of the nucleon-nucleon (NN) and three-nucleon (3N) interactions, derived from chiral effective field theory, have yielded major progress [1–3]. These, together with the utilization of massively parallel computing resources (e.g., see [4–6]), have placed *ab initio* large-scale simulations

Ch. Elster, R.B. Baker, G. Popa
Institute of Nuclear and Particle Physics, and Department of Physics and Astronomy, Ohio University, Athens, OH 45701, USA
E-mail: elster@ohio.edu

M. Burrows, K.D. Launey
Department of Physics and Astronomy, Louisiana State University, Baton Rouge, LA 70803, USA

S.P. Weppner
Natural Sciences, Eckerd College, St. Petersburg, FL 33711, USA

P. Maris
Department of Physics and Astronomy, Iowa State University, Ames, IA 50011, USA

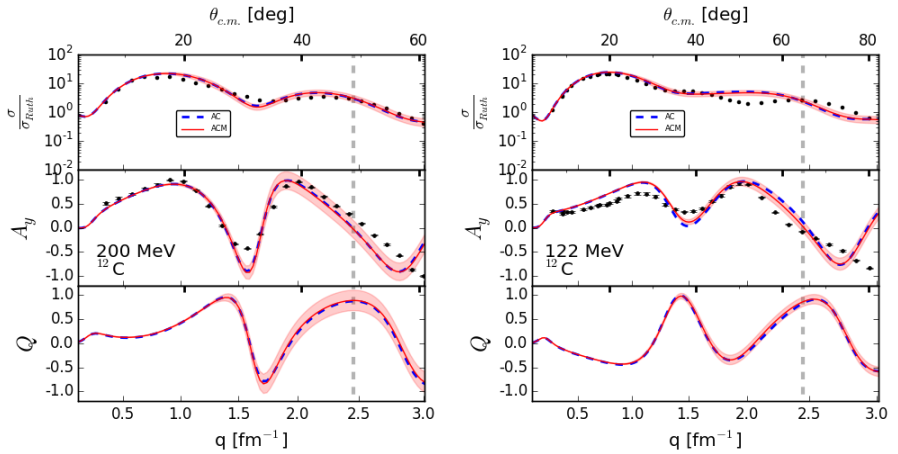

Fig. 1 Elastic scattering observables for proton scattering off ^{12}C at 200 MeV (left panel) and 122 MeV (right panel) projectile energy. Shown are the differential cross section divided by the Rutherford cross section, the analyzing power A_y and the spin-rotation function Q as function of the c.m. scattering angle $\theta_{c.m.}$as well as of the momentum transfer q. The grey dashed line represents the momentum transfer up to which the NNLO$_{\rm opt}$ chiral interaction [12] entering the calculations is fit to NN scattering data. The red solid line (ACM) represents the consistent leading order *ab initio* calculation of the effective interaction, while for the blue dashed line (AC) the spin of the struck target nucleon is ignored. The NCSM calculations use $N_{\rm max}$=10 and $\hbar\omega$=20. The red band represents the variation in the scattering observables when $\hbar\omega$=16 and 24 MeV are employed. The data are taken from Refs. [13] for 200 MeV and [14] for 122 MeV. This figure is taken from Ref. [15].

at the frontier of nuclear structure and reaction explorations. Here we focus on the use of the *ab initio* no-core shell model (NCSM) [7–9] and symmetry-adapted no-core shell model (SA-NCSM) [10,11] to provide the relevant structure inputs. Our approach to elastic nucleon-nucleus (NA) scattering is based on the spectator expansion of multiple scattering theory. Specifically, the leading order term in this expansion involves two-body interactions between the projectile and one of the target nucleons which requires a convolution of fully off-shell NN scattering amplitudes with the nuclear wave functions of the target represented by a nonlocal one-body nuclear density.

2 Nucleon-Nucleus effective interaction

The standard approach to elastic scattering of a strongly interacting projectile from a target of A particles using a multiple scattering approach is a separation of the Lippmann-Schwinger equation for the transition amplitude $T = V + VG_0(E)T$ into two parts, namely an integral equation for T and one for the effective potential U in the problem

$$T = U + UG_0(E)PT \quad \text{and} \quad U = V + VG_0QT. \tag{1}$$

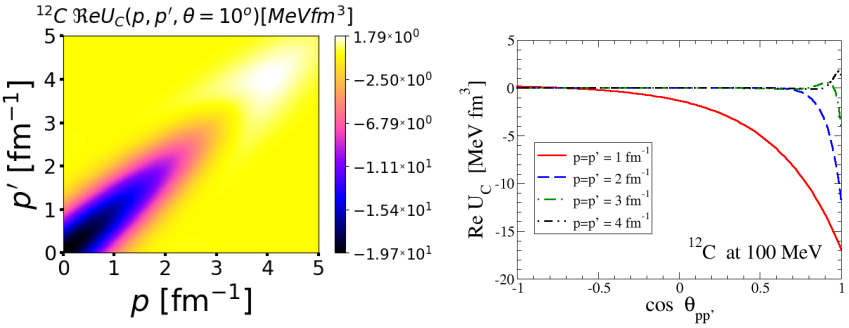

Fig. 2 The left panel shows the central effective potential for proton scattering off ^{12}C calculated for 100 MeV projectile energy as function of the momenta p and p' for fixed angle $\theta = 10^o$. The potential is based on the NNLO$_{\rm opt}$ chiral interaction [12]. The structure calculation employs $N_{\rm max}$=10 and $\hbar\omega$=20. The right panel depicts the angle dependence of the central effective potential for fixed values of $p = p'$ given in the legend.

In the above equations the operator $V = \sum_{i=1}^{A} v_{0i}$ consists of the NN potential v_{0i} acting between the projectile and the ith target nucleon. The free propagator $G_0(E)$ for the projectile+target system is given by $G_0(E) = (E - H_0 + i\epsilon)^{-1}$, and the Hamiltonian for the (A+1) particle system by $H = H_0 + V$. Here the free Hamiltonian is given by $H_0 = h_0 + H_A$, where h_0 is the kinetic energy operator for the projectile and H_A stands for the target Hamiltonian. Defining $|\Phi_A\rangle$ as the ground state of the target, we have $H_A|\Phi_A\rangle = E_A|\Phi_A\rangle$. The operators P and Q are projection operators, $P + Q = 1$. When considering elastic scattering P is defined such that $[G_0, P] = 0$.

The fundamental idea of the spectator expansion for the effective interaction is an ordering of the scattering process according to the number of active target nucleons interacting directly with the projectile. Thus in leading order only two active nucleons are considered. For the leading order term being *ab initio* means that the NN interaction for the active pair is considered at the same level as the NN interaction employed to obtain the ground state wave functions $|\Phi_A\rangle$. Details of the derivation of the leading order term and how the spin structure of the NN interaction is consistently taken into account in the reaction process are given in Refs. [15–17]. The resulting final expression for the *ab initio* leading order effective interaction is given as [18]

$$
\begin{aligned}
&\widehat{U}_{\rm p}(\boldsymbol{q}, \boldsymbol{\mathcal{K}}_{NA}, \epsilon) = \qquad (2)\\
&\quad \sum_{\alpha={\rm n,p}} \int d^3\mathcal{K}\eta\left(\boldsymbol{q}, \boldsymbol{\mathcal{K}}, \boldsymbol{\mathcal{K}}_{NA}\right) A_{{\rm p}\alpha}\left(\boldsymbol{q}, \overline{\boldsymbol{\mathcal{K}}_{\boldsymbol{A}}}; \epsilon\right) \rho_{\alpha}^{K_s=0}\left(\boldsymbol{\mathcal{P}'}, \boldsymbol{\mathcal{P}}\right)\\
&+ i(\boldsymbol{\sigma^{(0)}} \cdot \hat{\boldsymbol{n}}) \sum_{\alpha={\rm n,p}} \int d^3\mathcal{K}\eta\left(\boldsymbol{q}, \boldsymbol{\mathcal{K}}, \boldsymbol{\mathcal{K}}_{NA}\right) C_{{\rm p}\alpha}\left(\boldsymbol{q}, \overline{\boldsymbol{\mathcal{K}}_{\boldsymbol{A}}}; \epsilon\right) \rho_{\alpha}^{K_s=0}\left(\boldsymbol{\mathcal{P}'}, \boldsymbol{\mathcal{P}}\right)\\
&+ i \sum_{\alpha={\rm n,p}} \int d^3\mathcal{K}\eta\left(\boldsymbol{q}, \boldsymbol{\mathcal{K}}, \boldsymbol{\mathcal{K}}_{NA}\right) C_{{\rm p}\alpha}\left(\boldsymbol{q}, \overline{\boldsymbol{\mathcal{K}}_{A}}; \epsilon\right) S_{n,\alpha}\left(\boldsymbol{\mathcal{P}'}, \boldsymbol{\mathcal{P}}\right) \cos\beta
\end{aligned}
$$

$$+\, i(\boldsymbol{\sigma}^{(\mathbf{0})}\cdot\hat{\boldsymbol{n}})\sum_{\alpha=\mathrm{n,p}}\int d^3\mathcal{K}\eta\left(\boldsymbol{q},\boldsymbol{\mathcal{K}},\boldsymbol{\mathcal{K}}_{NA}\right)(-i)M_{\mathrm{p}\alpha}\left(\boldsymbol{q},\overline{\boldsymbol{\mathcal{K}}_A};\epsilon\right)S_{n,\alpha}\left(\boldsymbol{\mathcal{P}'},\boldsymbol{\mathcal{P}}\right)\cos\beta.$$

The term $\eta\left(\boldsymbol{q},\boldsymbol{\mathcal{K}},\boldsymbol{\mathcal{K}_{NA}}\right)$ is the Møller factor [19] describing the transformation from the NN frame to the NA frame, as is the term $\cos\beta$ [17]. The functions $A_{\mathrm{p}\alpha}$, $C_{\mathrm{p}\alpha}$, and $M_{\mathrm{p}\alpha}$ represent the NN amplitudes in the Wolfenstein representation [20]. Since the incoming proton can interact with either a proton or a neutron in the nucleus, the index α indicates the neutron (n) and proton (p) contributions, which are calculated separately and then summed up. With respect to the nucleus, the operator $i(\boldsymbol{\sigma}^{(\mathbf{0})}\cdot\hat{\boldsymbol{n}})$ represents the momentum space spin-orbit operator of the projectile. As such, Eq. (2) exhibits the expected form of an interaction between a spin-$\frac{1}{2}$ projectile and a target nucleus in a $J=0$ state [21]. The momentum vectors in the problem are given as

$$\begin{aligned}
\boldsymbol{q}=\boldsymbol{p'}-\boldsymbol{p}=\boldsymbol{k'}-\boldsymbol{k},\quad \boldsymbol{\mathcal{K}}=\frac{1}{2}\left(\boldsymbol{k'}+\boldsymbol{k}\right),\quad \hat{\boldsymbol{n}}=\frac{\boldsymbol{\mathcal{K}}\times\boldsymbol{q}}{|\boldsymbol{\mathcal{K}}\times\boldsymbol{q}|}\\
\boldsymbol{\mathcal{K}_{NA}}=\frac{A}{A+1}\left[\left(\boldsymbol{p'}+\boldsymbol{p}\right)+\frac{1}{2}\left(\boldsymbol{k'}+\boldsymbol{k}\right)\right],\quad \overline{\boldsymbol{\mathcal{K}}_A}=\frac{1}{2}\left(\frac{A+1}{A}\boldsymbol{\mathcal{K}}_{NA}-\boldsymbol{\mathcal{K}}\right),\\
\boldsymbol{\mathcal{P}}=\boldsymbol{\mathcal{K}}+\frac{A-1}{A}\frac{\boldsymbol{q}}{2},\quad \boldsymbol{\mathcal{P}'}=\boldsymbol{\mathcal{K}}-\frac{A-1}{A}\frac{\boldsymbol{q}}{2}.
\end{aligned}\tag{3}$$

The momentum dependence in Eq. (2) is quite intricate: Although the potential is needed in the (A+1)-body frame, its ingredients are derived in the NN frame as well as in the frame of the nucleus. A derivation and calculation based on the momentum transfer $\boldsymbol{q}$ and the momentum $\boldsymbol{\mathcal{K}_{NA}}$ are convenient due to the invariance of $\boldsymbol{q}$ in all frames. However, these variables may not be as intuitive for visualizing the potential. In this short contribution we want to concentrate on elastic proton scattering from ^{12}C using an *ab initio* effective potential based on the NNLO$_{\mathrm{opt}}$ chiral interaction [12] and a NCSM structure calculation based on the same interaction.

In Fig. 1 the elastic scattering observables, $d\sigma/d\Omega$ divided by the Rutherford cross section, analyzing power and spin rotation function, are shown for

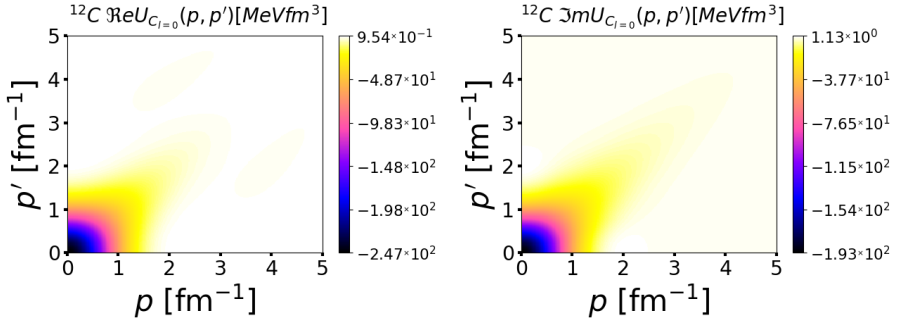

Fig. 3 The real (left panel) and imaginary (right panel) s-wave central effective potential for proton scattering off ^{12}C calculated for 100 MeV projectile energy as function of the momenta p and p'. The calculation is based on the same input as the one of Fig. 2.

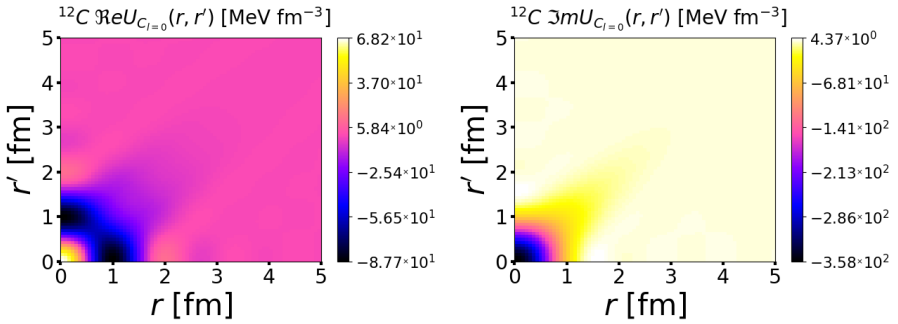

Fig. 4 Same as Fig. 3 but for the coordinate space s-wave central effective potential.

two different projectile energies and compared to existing data. The differential cross sections are very well described up to $q \sim 2$ fm^{-1}, as is the analyzing power at 200 MeV, while at 122 MeV it is slightly over-predicted at smaller q.

The effective interaction from Eq. (2) is nonlocal as well as energy dependent, and depends on two vector momenta. In order to visualize it in a more traditional form used in solving a momentum-space Lippmann-Schwinger equation, Fig. 2 depicts the real central part of the effective interaction as function of the momenta p and p' and an angle $\theta_{pp'} = 10^o$ together with the angle dependence at four different $p = p'$ values. The effective interaction is clearly peaked in forward direction. For Fig. 3 we perform a partial wave decomposition of the central part and show the s-wave contribution as function of p and p'. A Fourier transform leads to coordinate space representation of the central s-wave potential shown in Fig. 4. The radius obtained from the corresponding NCSM calculation of the ground state is about 2 fm. This is consistent with the figure showing the potential has its largest contributions for $r = r' \leq 2$ fm. It is also worthwhile to note that the largest negative contributions to the potential are not located along the line $(r + r')/2$.

3 Summary

In this short contribution we concentrate on elastic proton scattering off ^{12}C and a visualization of the *ab initio* effective interaction entering the calculation. The effective interaction is complex, nonlocal and a function of two vector momenta and the energy. We show the s-wave projected central part of the interaction in momentum as well as in coordinate space. The nonlocal structure of the real central s-wave effective potential for ^{12}C is quite similar in structure to the one described in Ref. [22] for the heavier nucleus ^{40}Ca, which is based on folding with a two-nucleon g-matrix. We also want to point out that the overall structure of the real s-wave potential from Fig. 4 has very similar characteristics to a real s-wave potential calculated from a Green's function approach combined with the coupled cluster approach for the nucleus ^{16}O [23].

Acknowledgements This work was performed in part under the auspices of the U. S. Department of Energy under contract Nos. DE-FG02-93ER40756 and DE-SC0018223, and by the U.S. NSF (OIA-1738287 & PHY-1913728). The numerical computations benefited from computing resources provided by Blue Waters (supported by the U.S. NSF, OCI-0725070 and ACI-1238993, and the state of Illinois), the Louisiana Optical Network Initiative and HPC resources provided by LSU, and resources of the National Energy Research Scientific Computing Center, a DOE Office of Science User Facility supported by the Office of Science of the U.S. Department of Energy under contract No. DE-AC02-05CH11231.

References

1. D.R. Entem, R. Machleidt, Phys. Rev. C **68**, 041001 (2003)
2. E. Epelbaum, Prog. Part. Nucl. Phys. **57**, 654 (2006)
3. E. Epelbaum, H.W. Hammer, U.G. Meissner, Rev. Mod. Phys. **81**, 1773 (2009). DOI 10.1103/RevModPhys.81.1773
4. D. Langr, I. Simecek, P. Tvrdik, T. Dytrych, J.P. Draayer, in *Proceedings of the Federated Conference on Computer Science and Information Systems (FEDCSIS), 2012* (2012), p. 545
5. H.M. Aktulga, C. Yang, E.G. Ng, P. Maris, J.P. Vary, Concurrency and Computation: Practice and Experience **26**(16), 2631 (2014). DOI 10.1002/cpe.3129
6. M. Jung, E.H. Wilson, III, W. Choi, J. Shalf, H.M. Aktulga, C. Yang, E. Saule, U.V. Catalyurek, M. Kandemir, in *Proceedings of the International Conference on High Performance Computing, Networking, Storage and Analysis* (ACM, New York, NY, USA, 2013), SC '13, pp. 75:1–75:11. DOI 10.1145/2503210.2503261. URL http://doi.acm.org/10.1145/2503210.2503261
7. P. Navratil, J.P. Vary, B.R. Barrett, Phys. Rev. Lett. **84**, 5728 (2000). DOI 10.1103/PhysRevLett.84.5728
8. R. Roth, P. Navratil, Phys. Rev. Lett. **99**, 092501 (2007). DOI 10.1103/PhysRevLett.99.092501
9. B. Barrett, P. Navrátil, J. Vary, Prog. Part. Nucl. Phys. **69**, 131 (2013)
10. K.D. Launey, T. Dytrych, J.P. Draayer, Prog. Part. Nucl. Phys. **89**, 101 (2016). DOI 10.1016/j.ppnp.2016.02.001
11. T. Dytrych, K.D. Launey, J.P. Draayer, D.J. Rowe, J.L. Wood, G. Rosensteel, C. Bahri, D. Langr, R.B. Baker, Phys. Rev. Lett. **124**(4), 042501 (2020). DOI 10.1103/PhysRevLett.124.042501
12. A. Ekström, G. Baardsen, C. Forssén, G. Hagen, M. Hjorth-Jensen, G.R. Jansen, R. Machleidt, W. Nazarewicz, et al., Phys. Rev. Lett. **110**, 192502 (2013)
13. H.O. Meyer, P. Schwandt, G.L. Moake, P.P. Singh, Phys. Rev. **C23**, 616 (1981). DOI 10.1103/PhysRevC.23.616
14. H.O. Meyer, P. Schwandt, W.W. Jacobs, J.R. Hall, Phys. Rev. **C27**, 459 (1983). DOI 10.1103/PhysRevC.27.459
15. M. Burrows, Ab initio leading order effective interactions for scattering of nucleons from light nuclei. Ph.D. thesis, Ohio University (2020)
16. M. Burrows, Ch. Elster, S.P. Weppner, K.D. Launey, P. Maris, A. Nogga, G. Popa, Phys. Rev. C **99**(4), 044603 (2019)
17. M. Burrows, R.B. Baker, Ch. Elster, S.P. Weppner, K.D. Launey, P. Maris, G. Popa, Phys. Rev. C **102**(3), 034606 (2020). DOI 10.1103/PhysRevC.102.034606
18. R.B. Baker, M. Burrows, C. Elster, K.D. Launey, P. Maris, G. Popa, S.P. Weppner, Phys. Rev. C **103**(5), 054314 (2021). DOI 10.1103/PhysRevC.103.054314
19. C. Møller, K. Dan. Vidensk. Sels. Mat. Fys. Medd. **23**, 1 (1945)
20. L. Wolfenstein, J. Ashkin, Phys. Rev. **85**, 947 (1952)
21. L. Rodberg, R. Thaler, *Introduction of the Quantum Theory of Scattering*. Pure and Applied Physics, Vol 26 (Academic Press, 1967)
22. H.F. Arellano, G. Blanchon, Phys. Rev. C **98**(5), 054616 (2018).
23. J. Rotureau, P. Danielewicz, G. Hagen, F.M. Nunes, T. Papenbrock, Phys. Rev. C **95**(2), 024315 (2017). DOI 10.1103/PhysRevC.95.024315